Available online at www.eccomasproceedia.org
Eccomas Proceedia SMART (2023) 935-946

ECCOMAS
Proceedia

X ECCOMAS Thematic Conference on Smart Structures and Materials
SMART 2023
D.A. Saravanos, A. Benjeddou, N. Chrysochoidis and T. Theodosiou (Eds)

MACHINE-LEARNING DRIVEN HEALTH MONITORING DIAGNOSTICS FOCUSED ON COMPOSITE STRUCTURES UTILIZING SMART LAYERWISE SPECTRAL ELEMENTS

CHRISTOFOROS REKATSINAS[*], GEORGE GIANNAKOPOULOS[*,†] AND VANGELIS KARKALETSIS[*]

[*] Software & Knowledge Engineering Lab, Institute of Informatics and Telecommunications, National Centre for Scientific Research "Demokritos", Greece
e-mail: crek@iit.demokritos.gr, https://www.iit.demokritos.gr

[†] Science For You - SciFY PNPC, Greece
email: ggianna @scify.org , www,scify.org

Abstract.
The present study discusses the value of a direct interaction between Structural Health Monitoring applications utilizing active piezoelectric sensors and Machine Learning algorithms in order to develop well established Artificial Intelligence driven diagnostics' tools for composite structures. More specifically, a high-fidelity Time Domain Spectral Finite Element model is developed incorporating physically modeled piezoelectric actuators and sensors as well as mixed order (linear and non-linear) Layerwise Mechanics to simulate efficiently the actual composite structure and all the respective failure modes (fiber, matrix failure and delamination) that could emerge within a composite material . The authors consequently planned a series of damage scenarios which could appear through the thickness of a composite laminate combining both intra- and inter- laminar damage. Afterwards, they simulated the respective virtual experiments of pitch and catch technique corresponding to the aforementioned scenarios by applying an actuating Guassian pulse and acquiring the respective responses of three sensors. Part of these data were then used as input to train different machine learning models predicting the composite material damage and classifying the damage type (output). We examine different approaches for representing the data to feed these machine learning models and present the very promising first findings regarding the effectiveness of the prediction, based on a cross-validation process on the generated simulation data.

Keywords: Structural Health Monitoring, Neural Networks, Mixed Order Layerwise Mechanics, Active Piezoelectric Sensors, Damage Classification, Guided waves, Intralaminar damage, Interlaminar damage, Machine Learning

Peer-review under responsibility of the organizing committee of SMART 2023.
doi: 10.7712/150123.9845.455509

1 INTRODUCTION

Composite structures are extensively used in various industries such as aerospace, automotive, and civil engineering, owing to their exceptional mechanical properties, such as high strength-to-weight ratio and corrosion resistance. However, these structures are susceptible to various types of damage caused by factors such as impact, fatigue, and environmental degradation [1]. Therefore, it is crucial to monitor their health continuously and detect any damage in a timely manner to ensure their safety and extend their service life. Structural health monitoring (SHM) is a technique that aims to achieve this objective by continuously monitoring the structural integrity of a system and detecting any damage or degradation [2], [3].

Smart materials, such as piezoelectric materials, are commonly used in SHM due to their ability to convert mechanical energy into electrical energy and vice versa, allowing for the detection of structural changes. In recent years, machine learning techniques, such as deep learning and convolutional neural networks, have been applied to *SHM* to improve the accuracy of damage detection and reduce false alarms [4].

One of the challenges of SHM is the accurate modeling of composite structures and the interpretation of sensor data. Spectral element methods, which use high-order polynomials to approximate the displacement field, have been shown to accurately model composite structures ([5], [6]). Additionally, smart layerwise spectral elements, which use piezoelectric sensors to monitor the health of composite structures, have been proposed ([7], [8]).

Several studies have been conducted in the area of SHM of composite structures using piezoelectric sensors ([9], [10]) This paper builds on previous works and extends it by utilizing machine learning algorithms for SHM applications [11], in combination with spectral element modeling and smart mixed order layerwise approach [12]. The proposed technique has the potential to provide an accurate and efficient approach to SHM of composite structures utilizing a small number of sensors, which can lead to significant improvements in the safety and durability of the structures.

In this article, we propose a machine-learning driven SHM technique focused on composite structures utilizing smart layerwise spectral elements. We demonstrate the effectiveness of our approach in detecting damage in composite structures using simulation data. We also compare the performance of our approach with other SHM techniques in the literature. The remainder of the paper is organized as follows: Section 2 discusses the spectral element method and the smart layerwise mechanics, Section 3 presents the proposed machine-learning driven SHM technique, Section 4 presents machine learning experiments based on simulation results, finally in the conclusion the paper discusses the potential aspects of the presented method and future work.

2 SMART MIXED ORDER SPECTRAL LAYERWISE ELEMENTS

Within the present section we describe the development and the implementation of a Mixed Order Smart Layerwise Time domain spectral element. The proposed numerical tool will be utilized to simulate active wave modulation in damaged composite plates. At the composite and cohesive layers we incorporated artificial damage (Figure 3) by introducing damage indexes

in the calculation of the stiffness matrix. Afterwards a 7-count excitation tone burst at 150kHz triggered both symmetric and antisymmetric guided waves. Finally, the captured sensor signals were used as input to the learning model in order to commence the training process and be able to identify future potential damage scenarios.

2.1 Mixed Order Smart Layerwise Mechanics

A variable kinematic layerwise theory is developed, which admits cubic variation of all displacements in the composite layers using Hermite polynomial splines [13] and is further enriched with linear discrete layers for the resin-rich interphase layers that admit linear variation of all displacements. The advantage of the described laminate layerwise mechanics is its potential to add and combine various discrete layers with variable thickness functions, which can be used to model laminated composite plates with interior interphase layers, as shown in Figure 1. Consequently, the through thickness approximation of displacements in each c^{th} composite layer or sublaminate is provided by one or more cubic discrete layers (CDL), as described below,

$$
\begin{aligned}
u_k(x,\mathrm{y},\zeta,\mathrm{t}) &= \mathbf{u}_k^1(x,y,\mathrm{t})\Psi_H^1(\zeta)+\mathbf{u}_k^2(x,y,\mathrm{t})\Psi_H^3(\zeta)+\mathbf{b}_k^1(x,y,\mathrm{t})\frac{h_k}{2}\Psi_H^2(\zeta)+\mathbf{b}_k^2(x,y,\mathrm{t})\frac{h_k}{2}\Psi_H^4(\zeta)\\
v_k(x,\mathrm{y},\zeta,\mathrm{t}) &= \mathbf{v}_k^1(x,y,\mathrm{t})\Psi_H^1(\zeta)+\mathbf{v}_k^2(x,y,\mathrm{t})\Psi_H^3(\zeta)+\mathbf{c}_k^1(x,y,\mathrm{t})\frac{h_k}{2}\Psi_H^2(\zeta)+\mathbf{c}_k^2(x,y,\mathrm{t})\frac{h_k}{2}\Psi_H^4(\zeta)\\
w_k(x,\mathrm{y},\zeta,\mathrm{t}) &= \mathbf{w}_k^1(x,y,\mathrm{t})\Psi_H^1(\zeta)+\mathbf{w}_k^2(x,y,\mathrm{t})\Psi_H^3(\zeta)+\mathbf{d}_k^1(x,y,\mathrm{t})\frac{h_k}{2}\Psi_H^2(\zeta)+\mathbf{d}_k^2(x,y,\mathrm{t})\frac{h_k}{2}\Psi_H^4(\zeta)\\
\varphi_k(x,\mathrm{y},\zeta,t) &= \boldsymbol{\varphi}_k^1(x,\mathrm{y},t)\Psi_H^1(\zeta)+\boldsymbol{\varphi}_k^2(x,\mathrm{y},t)\Psi_H^3(\zeta)+\mathbf{f}_k^1(x,\mathrm{y},t)\frac{h_k}{2}\Psi_H^2(\zeta)+\mathbf{f}_k^2(x,\mathrm{y},t)\frac{h_k}{2}\Psi_H^4(\zeta)
\end{aligned}
\tag{1}
$$

Similarly, $\boldsymbol{\varphi}_k^1, \boldsymbol{\varphi}_k^2, \mathbf{f}_k^1, \mathbf{f}_k^2$ denote the electric potential and its respective slopes at the top and bottom interfaces. Whereas the through-thickness approximation of the displacements in a thin RRL is assumed to be linear, thus, the interlaminar stresses are assumed constant. Hence, the respective in-plane and transverse displacement fields (*u, v, w*) for the r^{th} linear discrete layer (LDL) are approximated with linear interpolation functions by the following expressions,

$$
\begin{aligned}
u_r(x,\mathrm{y},\zeta,\mathrm{t}) &= u_r^1(x,y,\mathrm{t})\cdot\Psi_L^1(\zeta)+u_r^2(x,y,\mathrm{t})\cdot\Psi_L^2(\zeta)\\
v_r(x,\mathrm{y},\zeta,\mathrm{t}) &= v_r^1(x,y,\mathrm{t})\cdot\Psi_L^1(\zeta)+v_r^2(x,y,\mathrm{t})\cdot\Psi_L^2(\zeta)\\
w_r(x,\mathrm{y},\zeta,\mathrm{t}) &= w_r^1(x,y,\mathrm{t})\cdot\Psi_L^1(\zeta)+w_r^2(x,y,\mathrm{t})\cdot\Psi_L^2(\zeta)
\end{aligned}
\tag{2}
$$

In the previous equations, subscripts c and r indicate the CDL and LDL respectively, superscript i=1,2 denotes the bottom and top surface of each discrete layer, and $\Psi_H^i(\zeta)$, are the cubic Hermite splines and the linear Lagrange interpolation functions, which are given in Appendix A. Laminate mechanics description. As mandated by Eqs. (1)-(2) and illustrated in Figure 1, the continuity of the displacements across the common interface is self-satisfied, by using a common displacement for the top surface of the first DL and for the bottom surface of the second DL u_2^1, i.e., $u_1^2 = u_2^1 = u_2$.

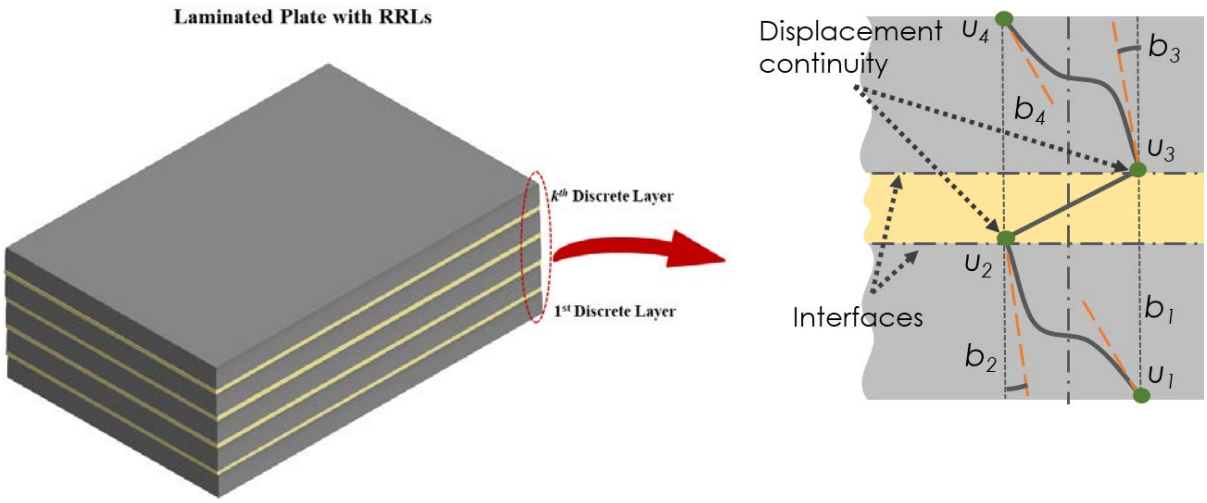

Figure 1. Schematic approximation of the displacement field and LW expansion for a multi-layer laminate with RRLs.

2.2 Time-domain spectral finite element model

The LW mechanics in conjunction with damage mechanics presented in the previous section, are used as a foundation for developing a multi-node plate finite element entailing C_0 Lagrange shape functions. The exploitation of high-order Lagrangian polynomial shape functions ensures the efficient spatial discretization in the plane of the plate. The nodes of the proposed element are collocated with Gauss-Lobatto-Legendre (GLL) integration points provided as solutions of the equations $\left(1-\xi_i^2\right)\cdot P_{p,\xi}\left(\xi_i\right)=0,\ \left(1-\eta_i^2\right)\cdot P_{p,\eta}\left(\eta_i\right)=0$, where $\xi,\eta\in[-1,1]$ are the local coordinates of the element. The generalized displacement and electric degrees of freedom are approximated in the plane of the element as follows,

$$\mathbf{U}_L(x,y,t)=\sum_{i=1}^{nodes}\mathbf{N}_u^i(x,y)\hat{\mathbf{U}}^i(t),\ \ \mathbf{\Phi}_L(x,y,t)=\sum_{i=1}^{nodes}\mathbf{N}_\varphi^i(x,y)\hat{\mathbf{\Phi}}^i(t) \tag{3}$$

where, overhat indicates the nodal displacements, superscript *i* denotes the corresponding node and **N** is the in-plane shape functions matrix.

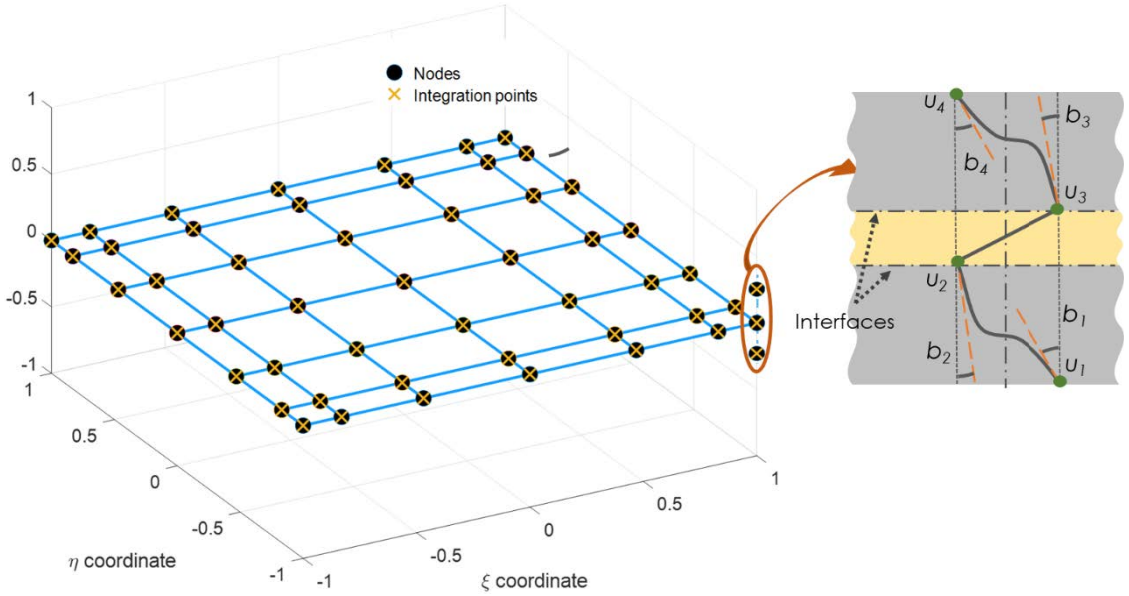

Figure 2. A 3D cohesive-layerwise spectral finite element model.

2.3 Problem description

In this sub-section, we describe the numerical application. More specifically, by utilizing the presented TDSFE, we simulated the guided wave propagation generated by an active piezoceramic patch in a damaged composite laminate. The examined case was a *[0, CL,90,CL,0]* CFRP composite plate, where CL stands for Cohesive Layer; the plate dimensions, the material properties and the actuation conditions were derived from the bibliography [14]. As Figure 5 shows, the developed MOSLM is in a very good agreement both in wave propagation speed and predicted sensor amplitude with the 3D continuum TDSFE.

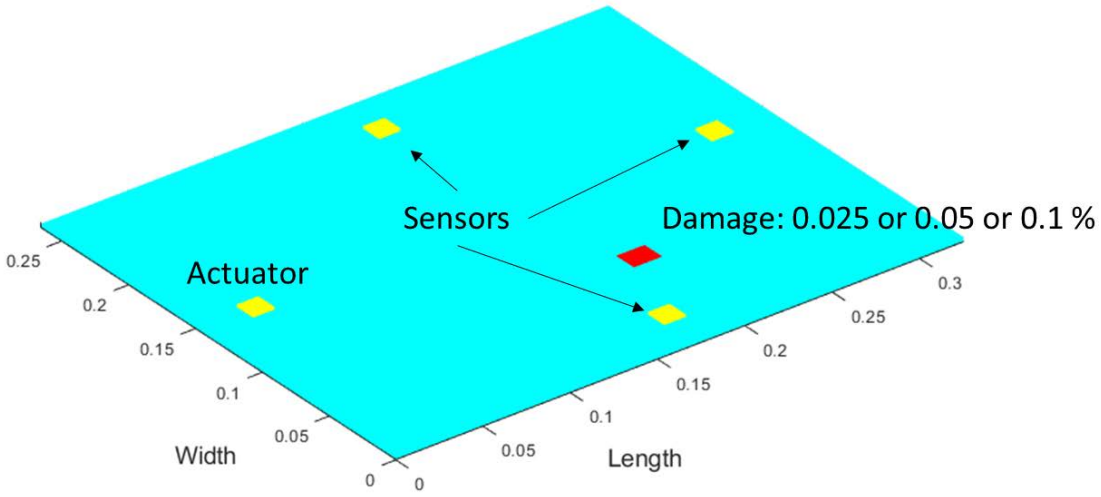

Figure 3. Visual representation of the carbon/epoxy composite plate with adhered PZTs and the incorporated damaged area.

3 MACHINE LEARNING DRIVEN SHM

Machine learning (ML) - and its subdomain of deep learning (DL) - has demonstrated significant contribution to natural sciences and engineering since it offers a capacity for data-driven discovery. This contribution is reflected on domains ranging from material design [15], to materials in archaeology [16], and to fiber reinforced composite manufacturing [17].

ML can have significantly different ways to support research endeavors, (indicatively) by:

- facilitating efficient (time-wise) and effective (precision-wise) identification of related work or datasets in a customized manner, according to research requirements;
- discovering complex relations between input parameters and functional results;
- allowing inverse design workflows, essentially suggesting the input parameters for a given functional result;
- speeding up costly calculations through approximation;
- reducing the number of required experiments to achieve a given outcome;
- facilitating characterization or index estimation for previously unseen data.

In this work we focus on the last point, by applying ML to estimate damage parameters, based on input from a set of appropriate sensors. These sensors provide time-series data, reflecting the effect of the damage on the selected material and structure. We, thus, pose the following questions in this SHM setting:

- Q1: Can ML be used to effectively predict such parameters and how accurate is it?
- Q2: How does one need to express and tackle the problem in ML terms, from the problem definition, to the data representation and the model used?
- Q3: How will such a model perform in the case of scarce data?

To this end we (a) examine different problem formulations of the parameter prediction task (classification or regression) - Q2; (b) examine different representations and their effect on the outcome of the prediction - Q2; (c) evaluate different ML (and DL) methods, from varying families of algorithms to estimate the required parameters, given the sensor input - Q1, Q3.

In the following paragraphs we describe the methodology as per the above aspects.

3.1 Problem formulation

Given that we want to predict a set of (numeric) parameters that characterize a given structure-damaging event, based on resulting multivariate sensor-based measurements (3 appropriately positioned sensors), we can follow two viewpoints for the prediction: formulating it as a regression or as a classification problem.

The regression viewpoint is the most straightforward way to approach the setting, allowing us to infer (from data) the function that connects the sensor input to the estimated parameter (output). We expect that the model will be able to provide accurate predictions on previously unseen data, essentially generalizing beyond the original observations. We stress that in this viewpoint the output prediction is numeric and essentially unbounded. Thus, the evaluation of such an approach relies on well-established functions, such as mean squared error (MSE) or mean absolute error (MAE).

The classification problem, on the other hand, requires a set of predefined labels plus a

training set, where we have labeled (also known as "annotated") observations, which are meant to guide the training of our model. Then, the model is expected to be able to label previously unseen data with one of the labels it has previously witnessed. This approach is more appropriate in controlled settings, where e.g. the damage parameter can only take specific discrete values. We note that in the dataset we generated, further described in the corresponding subsection, this discretization is in effect, allowing us to examine the classification viewpoint effectively.

To be able to apply classification, we need to convert the numeric parameters into class labels, which we achieve by simply treating numeric values as categorical values (thus, ignoring the ordering capacity that the numbers offer). The conversion of numeric parameters to (unordered, categorical) labels also implies that we cannot use regression-related accuracy metrics to evaluate our results. As an important side comment, to evaluate the performance of our prediction in a classification setting we can no longer utilize the MSE, MAE options. Instead, we utilize the accuracy, recall, precision and F1 measures [17].

To further explain the measures, we define the following setting. Given a number of N instances i_N that we examine, of which a belong to class A and b to class B, we consider that $P(i_N)$ is the prediction of the class of the i_N instance, based on our model. If i_N belongs to class A then, if $P(i_N)$=B we say that we have a false negative (FN) with respect to class A (FN_A). If $P(i_N)$=A, then we say that we have a true positive (TP) with respect to A (TP_A).

Considering the case that i_N belongs to A, if $P(i_N)$=B then $P(i_N)$ is a false positive (FP) with respect to class B (FP_B). Finally, in the case that i_N belongs to B, if $P(i_N)$=B, then $P(i_N)$ is a true negative (TN) with respect to class A (TN_A).

Given a table (termed confusion matrix) that shows the number of instances for each class and how they were assigned to classes by the prediction model, one case measure the following:

- the percentage of correct decisions that the predictor made, termed accuracy (AC).
- the percentage of instances of class X that the classifier predicted correctly, termed recall (RE).
- the percentage of the instances that were predicted as belonging to class X and were indeed of class X, termed precision (PR).
- the harmonic mean of precision and recall, termed F1(-score), which is high (i.e. close to 1) when both PR and RE are close to 1, but low otherwise.

We note that all the above measures are bounded between 0 and 1.

We now proceed to the part of the methodology which describes the ML selection considerations that will also guide our experiments in the corresponding section.

3.2 Representations and Models

In ML the selection of an appropriate representation for the input data is critical to the resulting performance. In this setting, we examine two main variations, given the fact that the data constitute a multivariate time series (3 signals from corresponding sensors): unchanged as 3D time series; feature vector based on the Fourier transform [18]. The latter representation is formed as follows:

- We calculate the discrete (1D) fourier transform of each of the 3 signals.

- We keep the N top contributing dimensions of the transform for each signal, essentially ending up with 3 vectors of size N.
- We concatenate the vectors into one single vection of 3N dimensions, representing the whole 3D signal.

We note that the representations also affect the prediction models we can use. Some regressors and classifiers work on feature vectors (which is the most typical use), while others (e.g. based on neural networks such as LSTM [19], or Hidden Markov Models, e.g.[20]).

Based on the above selected representations, we have tried various following models per formulation. Our selection of models was also guided by the scarcity of available data instances (which amount to a few tens). Due to this restriction, we focus on simple models, to avoid overfitting (i.e. creating models that cannot generalize to unseen data). The examined models (based on implementations in scikit-learn and pytorch [21] were as follows:

- Regression: (a) LSTM-based model[1] coupled with a multi-layer perceptron (MLP) for the final estimation - applicable on the time series representation; (b) Simple linear regression model - applicable on the Fourier-based representation; (c) LSTM-based model coupled with a multi-layer perceptron for the final class prediction - applicable on the time series representation.
- Classification: (a) k-Nearest Neighbor classifier (k=3); (b) Decision tree classifier.

In addition to the above methods, we add two baselines, one for the regression setting and the other for classification. The regression baseline is that of the average value of the training instances. The classification baseline is a "dummy" classifier using only prior probabilities of the labels in the training set to suggest labels (also called "stratified" dummy classifier), actually ignoring the input when making a decision on unseen data.

Having described the basic methodological decisions on the ML part of this work, we provide further information on the simulation that generated the dataset used to evaluate the ML methods.

4 Machine Learning Experiments

The experiments we conducted were meant to face the questions posed in the beginning of the methodology section (Q1, Q2, Q3). In the following paragraphs we overview the experimental results and map them to answers to these questions.

In Tables 1 and 2 we overview the performance of the different approaches in the regression and the classification approaches correspondingly. We note that the data included 35 instances (each containing a time series spanning 500 time points from 3 sensors), of which 13 reflected a damage level of 2.5%, 13 a level of 5% and 9 of 10% (thus imposing some class imbalance in the classification setting).

The evaluation is performed in a leave-one-out cross-validation manner: We perform 35 evaluations (folds), where on the i^{th} evaluation we train the predictive model on all but the i^{th} instance, which is used for evaluation. This allows us to also compute the standard error of the prediction accuracy in the classification case and similarly for the MAE in regression. In

[1] The details of the algorithm/model parameters are provided in the Appendix and can also be found in the project repository on Github.

regression, we also examine the (Spearman) correlation between the predictions and the real values, since a high such correlation shows that the prediction can be used as an index of the real value (regardless of the absolute difference).

On the other hand, the F1 is calculated on the confusion matrix of the total 35 folds. To average it we use a macro-average approach, i.e. we calculate the average of the F1 values with respect to all classes (without any weighting).

Representation	**Regression method**	**Mean Absolute Error** (lower is better)	**Spearman correlation (and p-value)**
3D time series	LSTM + MLP 1000 iterations, absolute error loss, Adam optimizer	0.0224	0.0815 (0.6418)
Fourier-based vector (100 dimensions per signal)	Simple linear	**0.0036**	**0.9387** (0.0000)
N/A	Baseline (average)	0.0246	-0.9453 (0.0000)

Table 1: Regression results. **Bold** letters indicate best performance.

Representation	**Algorithm / model**	**Accuracy** (higher is better)	**F1 (macro-average)** (higher is better)
3D time series	LSTM + MLP 1000 iterations, cross-entropy loss, Adam optimizer	0.1429 +/- 0.0591	0.1090
Fourier-based vector (100 dimensions per signal)	Decision Tree	0.8857 +/- 0.0538	0.8850
Fourier-based vector (100 dimensions per signal)	k-Nearest Neighbor (k=3)	**0.9143 +/- 0.0473**	**0.9152**
Fourier-based vector	Baseline - Dummy	0.4000 +/- 0.0828	0.3457

(100 dimensions per signal)	classifier - Stratification strategy		

Table 2: Classification results - **bold numbers** indicate best performance.

Based on the above tables we can see that: (a) ML appears to have significant potential for health monitoring diagnostics on composite structures. (Q1) (b) The above statement stands regardless of the actual formulation of the problem (classification or regression), which implies both approaches can be plausible and useful based on the setting. (Q2). (c) The prediction performance appears to sometimes be lower when using complex deep learning models on the sensor sequences, instead of using traditional Fourier transformation as feature generation from the sequences. Of course, this finding is also related to the scarcity of available data in our setting. Nevertheless, the selection of an appropriate representation and predictive model plays a significant role regarding the expected performance. (Q2) (d) Even with few instances (a few tens) the predictors appear to offer very promising prediction capability regarding the selected damage parameters. (Q3)

CONCLUSIONS

THIS WORK DEMONSTRATED SIGNIFICANT POTENTIAL IN HEALTH MONITORING OF COMPOSITE MATERIALS THROUGH THE USE of machine learning. However, in this study we demonstrated the value on a single damage parameter. As a natural next step comes the question: which parameters can be estimated sufficiently well through ML modeling and which, if any, cannot? Are still few data instances sufficient to model more complex settings and interactions? We need to study if the simple models that are sufficient in the presented case need to be replaced by more powerful (and complex) models if we mean to simultaneously predict sets of parameters regarding material health. We also need to examine further the optimizers of the deep learning models, since we noted (expected but non-optimal) behavior that leads to stagnation in the training and may lead to reduced prediction efficiency. Finally, we should more extensively examine how the system performs in previous unseen but also extreme events (outliers).

REFERENCES

[1] S. Abrate, "Impact on Laminated Composite Materials," *Appl. Mech. Rev.*, vol. 44, no. 4, p. 155, Apr. 1991, doi: 10.1115/1.3119500.

[2] A. Cuc, V. Giurgiutiu, S. Joshi, and Z. Tidwell, *Structural Health Monitoring with Piezoelectric Wafer Active Sensors for Space Applications*, vol. 45, no. 12. Elsevier/Academic Press, 2007.

[3] K. Diamanti, C. Soutis, and J. M. Hodgkinson, "Piezoelectric transducer arrangement for the inspection of large composite structures," *Compos. Part A Appl. Sci. Manuf.*, vol.

38, no. 4, pp. 1121–1130, 2007, doi: 10.1016/j.compositesa.2006.06.011.

[4] V. Giurgiutiu, "Tuned lamb wave excitation and detection with piezoelectric wafer active sensors for structural health monitoring," *J. Intell. Mater. Syst. Struct.*, vol. 16, no. 2, pp. 291–305, Apr. 2005, doi: 10.1177/1045389X05050106.

[5] C. S. Wang, J. H. Park, and F.-K. Chang, "Structures with Built-in Piezoelectric Sensor / Actuator Networks," no. July, 2015.

[6] C. S. Rekatsinas and D. A. Saravanos, "A Hermite Spline Layerwise Time Domain Spectral Finite Element for Guided Wave Prediction in Laminated Composite and Sandwich Plates," *J. Vib. Acoust.*, vol. 139, no. 3, p. 031009, Apr. 2017, doi: 10.1115/1.4035702.

[7] K. Lonkar and F. K. Chang, "Modeling of piezo-induced ultrasonic wave propagation in composite structures using layered solid spectral element," *Struct. Heal. Monit.*, vol. 13, no. 1, pp. 50–67, Jan. 2014, doi: 10.1177/1475921713500514.

[8] C. S. Rekatsinas, N. A. Chrysochoidis, and D. A. Saravanos, "Investigation of critical delamination characteristics in composite plates combining cubic spline piezo-layerwise mechanics and time domain spectral finite elements," *Wave Motion*, p. 102752, Apr. 2021, doi: 10.1016/j.wavemoti.2021.102752.

[9] N. A. Chrysochoidis and D. A. Saravanos, "High-frequency dispersion characteristics of smart delaminated composite beams," *J. Intell. Mater. Syst. Struct.*, vol. 20, no. 9, pp. 1057–1068, Jun. 2009, doi: 10.1177/1045389X09102983.

[10] W. Ostachowicz, M. Krawczuk, M. Cartmell, and M. Gilchrist, "Wave propagation in delaminated beam," *Comput. Struct.*, vol. 82, no. 6, pp. 475–483, Mar. 2004, doi: 10.1016/J.COMPSTRUC.2003.11.001.

[11] M. Moradi, A. Broer, J. Chiachío, R. Benedictus, T. H. Loutas, and D. Zarouchas, "Intelligent health indicator construction for prognostics of composite structures utilizing a semi-supervised deep neural network and SHM data," *Eng. Appl. Artif. Intell.*, vol. 117, p. 105502, Jan. 2023, doi: 10.1016/J.ENGAPPAI.2022.105502.

[12] D. Siorikis, "A layerwise spectral finite element method for the prediction of stresses and delamination crack growth in composite structures subjected to static and impact loading," University of Patras; Department of Mechanical and Aeronautical Engineering, 2022.

[13] D. K. K. Siorikis, C. S. S. Rekatsinas, N. A. A. Chrysochoidis, and D. A. A. Saravanos, "A cubic spline layerwise spectral finite element for robust stress predictions in laminated composite and sandwich strips," *Eur. J. Mech. A/Solids*, vol. 91, no. June

2021, p. 104362, Jul. 2022, doi: 10.1016/j.euromechsol.2021.104362.

[14] C. S. C. S. S. Rekatsinas and D. A. D. A. A. Saravanos, “A cubic spline layerwise time domain spectral FE for guided wave simulation in laminated composite plate structures with physically modeled active piezoelectric sensors,” *Int. J. Solids Struct.*, vol. 124, pp. 176–191, Oct. 2017, doi: 10.1016/j.ijsolstr.2017.06.031.

[15] P. Krokidas *et al.*, “Data mining for predicting gas diffusivity in zeolitic-imidazolate frameworks (ZIFs),” *J. Mater. Chem. A*, vol. 10, no. 26, pp. 13697–13703, Jul. 2022, doi: 10.1039/D2TA02624D.

[16] S. H. Bickler, “Machine Learning Arrives in Archaeology,” *Adv. Archaeol. Pract.*, vol. 9, no. 2, pp. 186–191, May 2021, doi: 10.1017/AAP.2021.6.

[17] M. Priyadharshini, D. Balaji, V. Bhuvaneswari, L. Rajeshkumar, M. R. Sanjay, and S. Siengchin, “Fiber Reinforced Composite Manufacturing With the Aid of Artificial Intelligence – A State-of-the-Art Review,” *Arch. Comput. Methods Eng.*, vol. 29, no. 7, pp. 5511–5524, Nov. 2022, doi: 10.1007/S11831-022-09775-Y/FIGURES/6.

[18] Z. Wang, “Fast Algorithms for the Discrete W Transform and for the Discrete Fourier Transform,” *IEEE Trans. Acoust.*, vol. 32, no. 4, pp. 803–816, 1984, doi: 10.1109/TASSP.1984.1164399.

[19] F. Karim, S. Majumdar, H. Darabi, and S. Chen, “LSTM Fully Convolutional Networks for Time Series Classification,” *IEEE Access*, vol. 6, pp. 1662–1669, Sep. 2017, doi: 10.1109/ACCESS.2017.2779939.

[20] J. Li, A. Najmi, and R. M. Gray, “Image classification by a two-dimensional hidden Markov model,” *IEEE Trans. Signal Process.*, vol. 48, no. 2, pp. 517–533, 2000, doi: 10.1109/78.823977.

[21] A. Paszke *et al.*, “PyTorch: An Imperative Style, High-Performance Deep Learning Library,” *Adv. Neural Inf. Process. Syst.*, vol. 32, Dec. 2019, Accessed: May 08, 2023. [Online]. Available: https://arxiv.org/abs/1912.01703v1.